Dual-band and Tri-band Balanced-to-Single-Ended Power Dividers with Wideband Common-mode Suppression

He Zhu, *Member, IEEE*, and Y. Jay Guo, *Fellow, IEEE*

***Abstract*—A new design approach of developing multi-band balanced-to-single-ended (BTSE) power dividers is presented in this paper. The design is based on flexible coupling schemes which can guide designing multi-band balanced-to-single-ended power dividers with arbitrary number of bands and controllable bandwidth. Microstrip-to-slotline transitions are used to suppress the transmission of common-mode signals at all frequencies, which lead to an ultra-wide bandwidth of common-mode suppression. Slotlines play a critical role for they have two functions, one is to control the external coupling between ports and resonators, and the other one is to prohibit the propagation of common-mode signals. Based on the design approach, a dual-band and a tri-band balanced-to-single-ended power divider are modeled and simulated in the EM simulation environment. Prototypes are fabricated and tested, and the experimental results demonstrate that dual-band and tri-band filtering responses are realized in a BTSE power divider design. Moreover, the common-mode suppression and mode conversion levels of both designs are less than -29.5 dB at all frequencies (common-mode suppression fractional bandwidth is 200%), which is extremely desired in differential circuits and systems.**

***Index Terms*—Balanced-to-single-ended, coupling scheme, common-mode suppression, dual-band, filtering response, multi-band, power dividers, tri-band, slotline.**

I. Introduction

DIFFERENTIAL signals and circuits have the advantages of high immunity to electromagnetic interference and environmental noises, so that a series of balanced microwave components are required in wireless communication systems. These include balanced bandpass filters [1]-[3], balanced power dividers [4]-[6], balanced couplers [7]-[8], balanced phase shifters [9], etc. Among these balanced components, balanced power dividers are widely used for they can split signals into several parts and convert them between balanced and unbalanced states. Balanced-to-single-ended (BTSE) power dividers are able to convert balanced signals into unbalanced signals and split them into two parts, and thus they are usually used in a RF front-end to connect with a differentially-fed antenna. Some designs were presented in the literature [10]-[12]. In a typical RF front-end, bandpass filters are usually connected with power dividers, and thus in order to make the design more compact and multi-functional, filtering responses were considered in BTSE power divider designs, such as in [13]-[15]. In [15], a wideband filtering BTSE power divider was realized using slotline resonators, and an ultra-wide bandwidth of CM suppression was also obtained.

Multiband balanced-to-single-ended power dividers are demanded as they can select signals at different frequencies and divide these signals to two paths. These signals may contain multiple frequencies which are used in different scenarios, so the multiband BTSE power divider usually connect with a balanced multiplexer, which can combine the signals at all frequencies from channel 1 to channel *n*, as shown in Fig. 1. For the multiband BTSE power divider, it comprises of a pair of balanced ports Port A^+ and A^- and two single-ended output ports Port 2 and 3. Fig. 2 indicates that a traditional multiband BTSE power divider is realized by cascading a balun with a multiband filter and a single-ended power divider. In this case, the overall size of three components would be very bulky. A dual-band BTSE power divider design was introduced in [16], which realized dual-band filtering response and good in-band common-mode suppression.

An existing problem is that it is quite difficult to make the number of channels more than two as only dual-band BTSE power divider designs were found. However, in some scenarios, tri-band or even more channel designs are needed. Although tri-band balanced bandpass filters were presented before such as in [17]-[18], tri-band balanced power dividers were never investigated. This work, for the first time, presents a tri-band BTSE power divider with excellent common-mode suppression capability. Instead of using traditional bulky size of cascaded components, this work introduces a very compact structure of a dual-band and a tri-band BTSE power divider design based on a universal design approach using coupling schemes. This design method is very flexible as the position and bandwidth of each band can be easily controlled based on the selected coupling scheme. Besides, the issue of common-mode rejection capability is also considered as an ultra-wide common-mode rejection bandwidth is obtained. To verify this method, a dual-band and a tri-band BTSE power divider are designed, simulated and tested. The experimental result agrees with the predicted one, demonstrating that the design method is very useful in the development of multiband BTSE power dividers.

Manuscript submitted July 23, 2020.

The authors are with the Global Big Data Technologies Center (GBDTC), University of Technology Sydney, Ultimo, NSW 2007, Australia. (email: he.zhu@uts.edu.au)

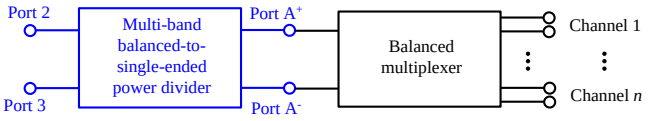

Fig. 1. Diagram of a multiband BTSE power divider in a balanced transceiver.

Fig. 2. Diagram blocks of a traditional multiband BTSE power divider.

II. Dual-Band BTSE Power Divider

A. Coupling Scheme

Traditional way of building dual-band balanced-to-single-ended power dividers is to convert the unbalanced signals to balanced signals and then divide the signal into two paths. Usually the filtering characteristics are added by loaded stubs or other structures, but in this case, the selection of band ratio is limited in a small range and the bandwidth of two bands is difficult to be controlled separately. To make the design flexible, it is desired to have arbitrary position and full control of bandwidth at each band. Moreover, the isolation of all bands between output ports is hard to handle, so an extra isolation circuit is usually required. This isolation circuit should be located at the center point between two output ports to avoid any effect on the odd-mode circuit.

In this section, a new type of coupling scheme will be presented to develop filtering characteristics in multiband balanced-to-single-ended power dividers. A diagram of such coupling scheme for a dual-band design is given in Fig. 3. A pair of balanced ports S and S' are connected with a non-resonating node N_0, and then it connects with two pairs of resonators. The resonators R_1 and R'_1, R_2 and R'_2 should be selected at the resonant frequency f_1 and f_2. Another non-resonating node N_1 is used to connect two unbalanced ports L_1 and L_2. Since all selected bands are quite narrow, it is crucial to control the external quality factor of the filtering response. In this case, the non-resonating node N_0 is responsible for controlling the external quality factors Q_{e1} and Q_{e2} at the input port, Q_{e1} and Q_{e2} denote the external quality factors of two bands. Similarly, the non-resonating node N_0 is responsible for controlling the external quality factors Q'_{e1} and Q'_{e2} at two output ports. The mutual coupling of each band is regarded as M_1 and M_2, which is controlled by the coupling factor between two resonators. It is noted that the issue of isolation and output matching is not considered here. It can be realized by an extra circuit connected tonon-resonating node N_1 without affecting the transmitting performance of differential-mode signals.

B. Design and Analysis

To convert the balanced signals to unbalanced signals, 180° transmission lines are usually used to connect two balanced ports. The problem of this method is that the bandwidth of common-mode (CM) rejection is quite limited as the common-mode rejection band is only located within the

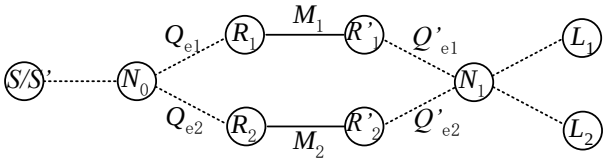

Fig. 3. Coupling scheme of a dual-band BTSE power divider.

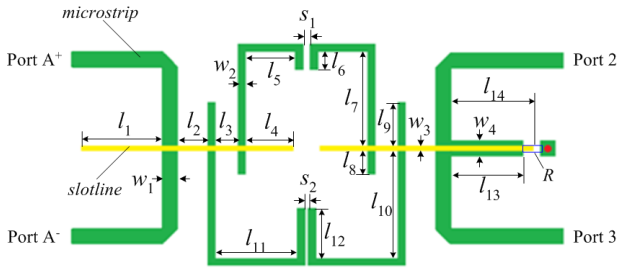

Fig. 4. Layout of the proposed dual-band balanced-to-single-ended power divider.

passband range. It is more desired that the common-mode signals at all frequencies can be prohibited. To this end, methods like slotlines can be adopted in balanced power divider designs because they can effectively suppress the common-mode signals, for the electrical field distribution of the propagation mode does not support the common-mode signals.

Fig. 4 shows the overall design layout of the proposed dual-band BTSE power divider using a single-layer substrate. In this design, slotlines function as non-resonating nodes for they have multiple functions, including common-mode rejection, mode conversion and controlling external coupling. To convert unbalanced signals to balanced signals, balanced-microstrip-to-slotlines transitions are used to transmit balanced signals from microstrip lines into slotlines [15]. Microstrip resonators are coupled with slotlines via microstrip-to-slotline transitions. It is noted that the coupling area will affect the external quality factor so it is flexible to control the length of the microstrip line to get a suitable external coupling factor. For two pairs of microstrip resonators, the resonance will occur at the frequency of

$$f_1 = \frac{c}{4(L_5 + L_6 + L_7 + L_8)\sqrt{\varepsilon_r}} \quad (1)$$

$$f_2 = \frac{c}{4(L_9 + L_{10} + L_{11} + L_{12})\sqrt{\varepsilon_r}} \quad (2)$$

where c refers to the speed of light and ε_r is the relative permittivity of the substrate.

Besides, the coupled-line section area determines the coupling coefficient, which means it is possible to get a flexible in-band ripple level by tuning the coupling factor of the coupled-line section. The coupling coefficient can be obtained using the following equation:

$$M_i = \frac{f_{p2}^2 - f_{p1}^2}{f_{p2}^2 + f_{p1}^2} \qquad i = 1,2 \quad (3)$$

where f_{p2} and f_{p1} refer to the higher and lower resonant frequencies of resonators within each band. To adjust the value of M_1 and M_2, it is possible to tune the gap distance s_1 and s_2.

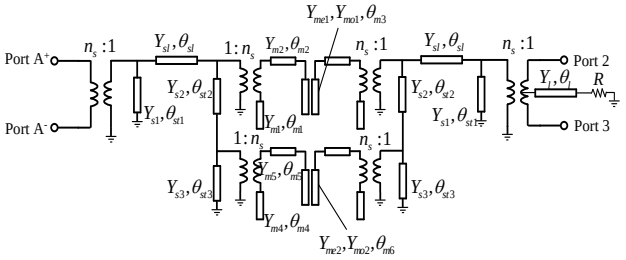

Fig. 5. Equivalent circuits of the proposed dual-band balanced-to-single-ended power divider.

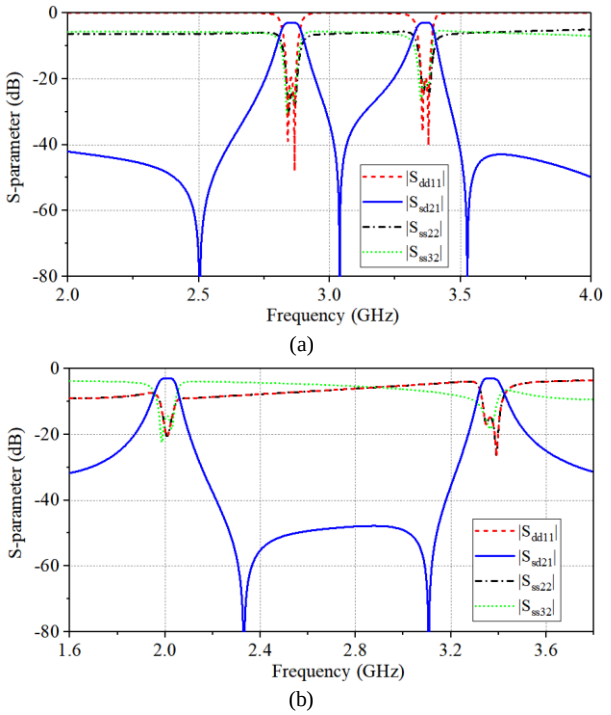

Fig. 6. Synthesized results of two BTSE power divider designs using equivalent circuit: (a) Design-I (associated parameters are: Z_{s1}=Z_{s2}=Z_{s3}=Z_{sl}=105.3 Ω, Z_{m1}=123.2 Ω, Z_{me1}=98.9 Ω, Z_{mo1}=82.8 Ω, Z_{me2}=104.8 Ω, Z_{mo2}=71.5 Ω, Z_l=32.8 Ω, R=43 Ω, θ_{s1}=62.8°, θ_{s2}=7.6°, θ_{s3}=46.6°, θ_{sl}=24.3°, θ_{m1}=35.1°, θ_{m2}=65.7°, θ_{m3}=25.2°, θ_{m4}=30.6°, θ_{m5}=39.8°, θ_{m6}=87.9°, θ_l=90°, n_s=0.85, f_o=2.4 GHz); Design-II (associated parameters are: Z_{s1}=Z_{s2}=Z_{s3}=Z_{sl}=109.8 Ω, Z_{m1}=106.8 Ω, Z_{me1}=91.9 Ω, Z_{mo1}=75.5 Ω, Z_{me2}=115.7 Ω Z_{mo2}=74 Ω, Z_l=38.3 Ω, R=58 Ω, θ_{s1}=72.7°, θ_{s2}=39.8°, θ_{s3}=26.6°, θ_{sl}=24.3°, θ_{m1}=70.5°, θ_{m2}=60.3°, θ_{m3}=18°, θ_{m4}=28.8°, θ_{m5}=24°, θ_{m6}=112.2°, θ_l=90°, n_s=0.85, f_o=2.4 GHz).

The external quality factors Q_{e1} and Q_{e2} are controlled by the length of l_8 and l_9, and longer l_8 and l_9 will lead to stronger external coupling of the filter. Regarding the output ports, in order to get perfect matching at two single-ended ports and ideal isolation between two ports, an extra isolation circuit consisting of a stub loaded with a grounded resistor is added at the center point of two output ports. To make two output ports matched within all bands, the length of the stub is selected as quarter-wavelength at center frequency f_0.

An equivalent circuit of the design is shown in Fig. 5 to analyze the filtering characteristics in the differential-mode (DM) circuit of the design. The microstrip-to-slotline transition is modeled by a transformer with turn ratio of n_s, and its typical value is around 0.85. The external coupling is affected by the length of θ_{st2} and θ_{st3}. The length of (θ_{m1} + θ_{m2} + θ_{m3}) determines the first resonance and the length of (θ_{m4} + θ_{m5} + θ_{m6}) deter-

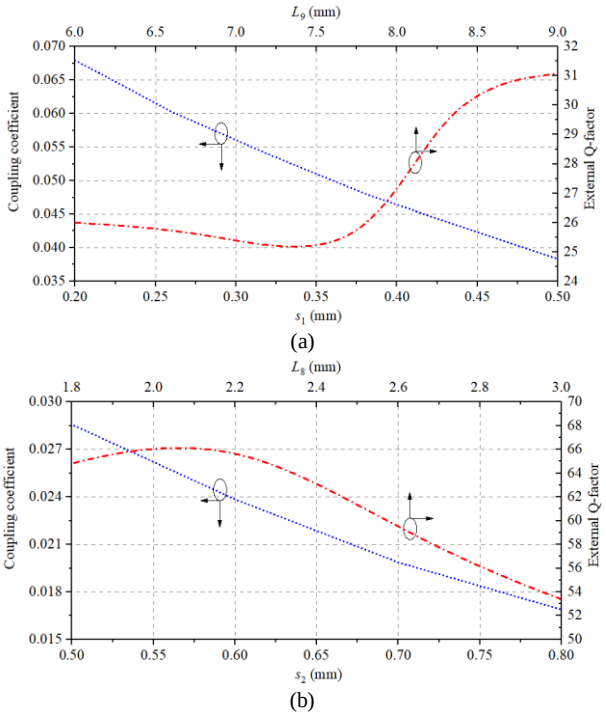

Fig. 7. Coupling coefficient and external quality factor of two bands against the related parameters s_1, s_2, L_8 and L_9.

mines the second resonance. The in-band coupling coefficient is related to the coupling factor of (Z_{me1}, Z_{mo1}) and (Z_{me2}, Z_{mo2}). To get perfect matching and ideal isolation between output ports, it is required that

$$Z_o = 2Z_l \cdot \frac{2R + j \cdot 2Z_l \tan\theta_l}{2Z_l + j \cdot 2R \tan\theta_l} \tag{4}$$

Since $\theta_l = 90°$ at the center frequency, the resistance of R can be found to be $R = 2Z_l^2/Z_o$. It is noted that when even-mode excitations are applied at Port A$^+$ and Port A$^-$, the center line of the transformer would become a virtual magnetic wall which works as open circuit. In this case, the transformer will not work so that signals would be terminated. This explains that the common-mode signals are rejected and totally reflected at the microstrip-to-slotline transition. On the other hand, when odd-mode signals excitations are applied at Port A$^+$ and Port A$^-$, the center line of the transformer would become a virtual electrical wall which works as short circuit. This odd-mode circuit would support the transmission of differential-mode signals and provide a multi-band filtering response.

Based on the equivalent circuit, two balanced-to-single-ended power divider designs are simulated, and the simulation results are displayed in Fig. 6(a) and (b), respectively. It is seen that for the differential-mode signals, multiple transmission zeros can be produced at the edges of two bands, including one or two transmission zeros between them. To make the design simpler, the impedances of each microstrip line and slotline are selected as a fixed value. The common-mode transmission and DM-to-CM mode-conversion level are equal to 0 at all frequencies, indicating an ultra-wide CM suppression bandwidth of the design. It is noted that the frequency ratio f_2/f_1 can be tuned in a wide range.

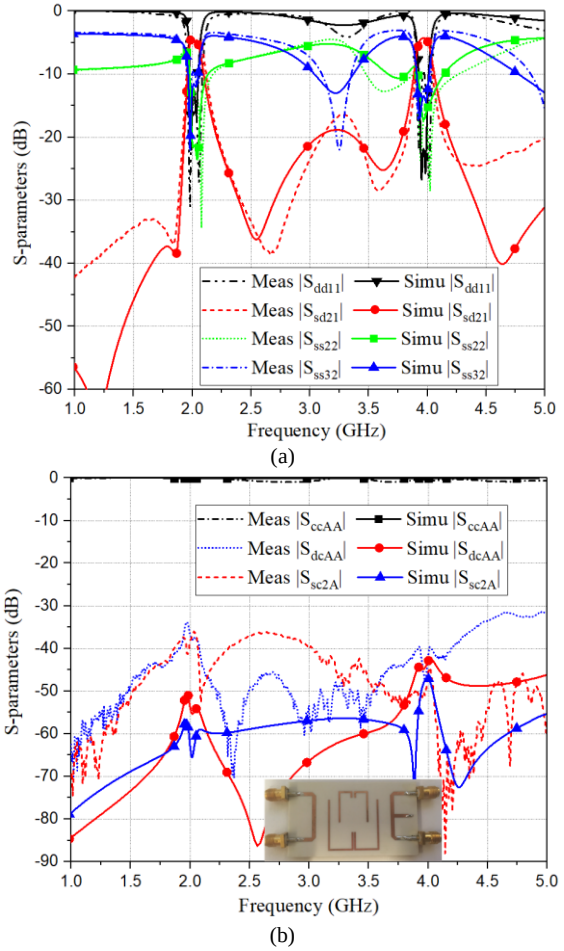

Fig. 8. Measured and simulated results of the dual-band BTSE power divider: (a) $|S_{ddAA}|$, $|S_{sd2A}|$, $|S_{ss22}|$ and $|S_{ss32}|$; (b) $|S_{ccAA}|$, $|S_{dcAA}|$ and $|S_{sc2A}|$.

C. Experiment Verification

Full-wave simulation of the model in Fig. 4 is done using EM simulation environment to verify the dual-band BTSE power divider design. The selected substrate is Rogers RO4350b with dielectric constant of 3.48 and thickness of 0.76 mm. The physical lengths of two pair of resonators are found from (1) and (2). The coupling coefficient and external quality factor of each band are controlled by the gap distance s_1 and s_2 between two resonator pairs and the length of L_8 and L_9, respectively, and their relationships are extracted in Fig. 7. In the design, the center frequency of two bands is 2 GHz and 4 GHz, respectively, and f_0 is chosen to be 3 GHz. The required values of M_1, M_2, Q_{ex1} and Q_{ex2} are 0.05, 0.025, 28 and 56, so that the desired dimensions can be found in Fig. 7.

After EM simulation is done in full-wave simulation environment, the dimensions in the layout are found to be: L_1= 6.7, L_2= 2.3, L_3= 1.7, L_4= 4.7, L_5= 6.5, L_6= 2.8, L_7= 10.6, L_9= 3.2, L_{10}= 16.4, L_{11}= 8.7, L_{12}= 6.7, L_{13}= 8.7, L_{14}= 9.8, w_1= 1.7, w_2= 0.6, w_3= 0.4, w_4= 1.8, s_1= 0.2, s_2= 0.6, all in mm. The isolation resistor is chosen as 47 Ω. Fig. 8 shows the simulated and measured results of a fabricated prototype. The measured insertion loss of two bands is 2.0 dB and 1.8 dB, and the measured bandwidth of two bands is 7.14% and 3.21, respectively. The measured common-mode level and the mode-conversion level are below -32 dB at all frequencies. These results proved that the design realized a wide CM suppression bandwidth.

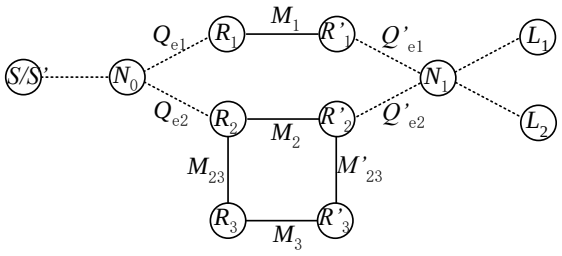

Fig. 9. Coupling scheme of a tri-band balanced-to-single-ended power divider.

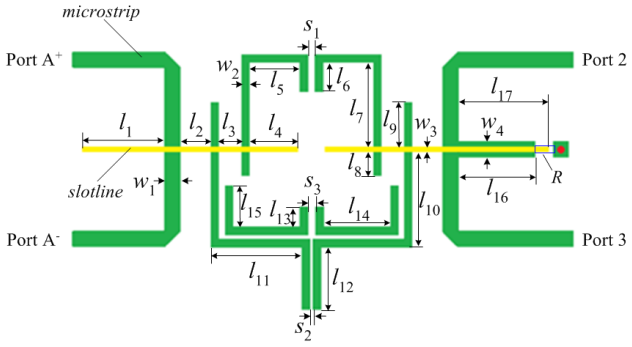

Fig. 10. Layout of the proposed tri-band balanced-to-single-ended power divider.

III. Tri-Band BTSE Power Divider

A. Design and Simulation

In this section, a tri-band balanced-to-single-ended power divider will be presented. The coupling scheme of such design is shown in Fig. 9. Compared with the dual-band design, the tri-band design has another pair of resonators R_3 and R'_3, which are coupled to R_2 and R'_2 via electrical coupling. In this case, the external quality factor of the third band is the same with the second one. Actually the third pair of resonators can be connected with the non-resonating nodes N_0 and N_1 as well, but this will lead to some problems including less independence of bandwidth control and difficulties in building physical layout. Due to the existence of cross coupling M_{23} and M'_{23}, two additional transmission zeros between adjacent bands will also be introduced.

Based on the coupling scheme, a tri-band BTSE power divider is built using a single-layer substrate as shown in Fig. 10. The third band is better to be chosen at a higher frequency, because the length of the third resonator pair needs to be short enough to fulfill layout design requirement. The external coupling factor is tuned by the gap distance s_4 between the second and third resonator pairs. It is noted that the matching and isolating circuit at the output ports is also the same with the dual-band design.

B. Experiment Verification

Full-wave simulation of the model in Fig. 10 is also done in EM simulation environment to verify the design. The three bands are selected at 2.4 GHz, 3.5 GHz and 5.2 GHz, and the frequency ratio is 2.2:1.5:1. Same substrate is adopted with the dual-band design. The dimensions for the tri-band power

divider are found to be: L_1= 6.7, L_2= 2.3, L_3= 1.7, L_4= 4.7, L_5= 6.5, L_6= 2.8, L_7= 10.6, L_9= 3.2, L_{10}= 16.4, L_{11}= 8.7, L_{12}= 6.7,

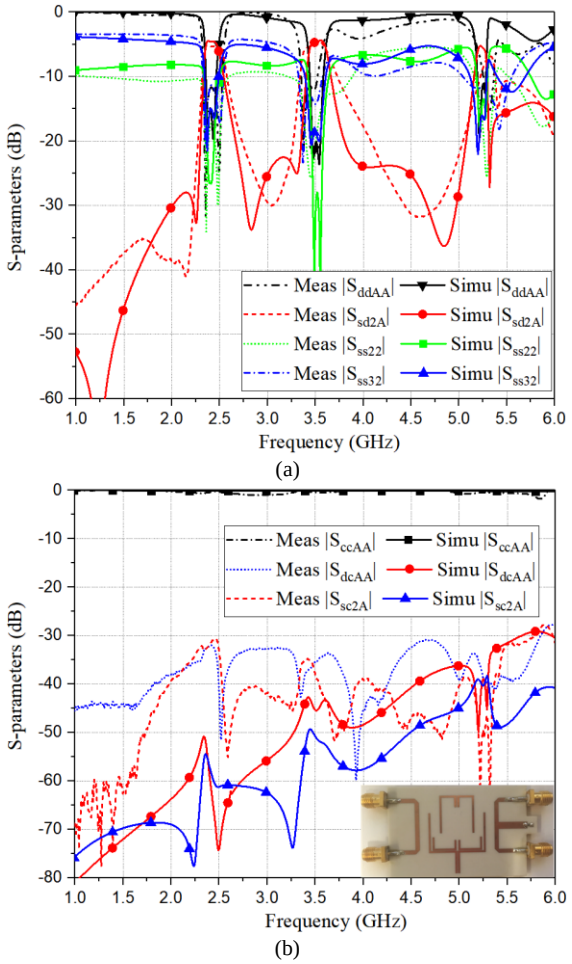

Fig. 11. Measured and simulated results of the tri-band BTSE power divider: (a) $|S_{ddAA}|$, $|S_{sd2A}|$, $|S_{ss22}|$ and $|S_{ss32}|$; (b) $|S_{ccAA}|$, $|S_{dcAA}|$ and $|S_{sc2A}|$.

L_{13}= 8.7, L_{14}= 9.8, L_{15}= 8.7, L_{16}= 9.8, w_1= 1.7, w_2= 0.6, w_3= 0.4, w_4= 1.8, s_1= 0.2, s_2= 0.6, s_3= 0.3, s_4= 0.5, all in mm. The isolation resistor is chosen as 47 Ω.

Fig. 11 shows the simulated and measured results of a fabricated prototype. The return loss of the balanced input port and output ports is less than -11 dB and -13 dB, and the isolation between port 2 and 3 is -15 dB. Multiple transmission zeros are produced at two edges of each band. The measured CM transmission and mode-conversion level are less than -29.5 dB at all frequencies. Small discrepancies are caused by the fabrication error of the prototype. The experiment results of two designs have verified the design approach successfully.

IV. Conclusion

A dual-band and a tri-band balanced-to-single-ended power divider have been presented in this paper. Both of two designs are developed based on a new method using coupling scheme to realize multi-band filtering response in the differential-mode transmission characteristics. Meanwhile, regarding the common-mode performance, an ultra-wide bandwidth of common-mode suppression has been achieved at a very low level of less than -29.5 dB at all frequencies. This is realized by slotlines and microstrip-to-slotline transitions. Two prototypes are fabricated and tested, and the experiment results revealed that multi-band filtering responses and wideband common-mode suppression capability are realized successfully.

References

[1] X. Bi, X. Zeng, and Q. Xu, "Slotline-based balanced filter with ultra-wide stopband and high selectivity," *IEEE Trans. Circuits Syst. II, Exp. Briefs*, vol. 67, no. 3, pp. 460–464, Mar. 2020.

[2] R. Gómez-García, R. Loeches-Sánchez, D. Psychogiou, and D. Peroulis, "Multi-stub-loaded differential-mode planar multiband bandpass filters," *IEEE Trans. Circuits Syst. II, Exp. Briefs*, vol. 65, no. 3, pp. 271–275, Mar. 2018.

[3] H. Zhu and A. M. Abbosh, "Tunable balanced bandpass filter with wide tuning range of center frequency and bandwidth using compact coupled-line resonator," *IEEE Microw. Wireless Compon. Lett.*, vol. 26, no. 1, pp. 7–9, Jan. 2016.

[4] W. Feng et al., "Multi-functional balanced-to-unbalanced filtering power dividers with extended upper stopband," *IEEE Trans. Circuits Syst. II, Exp. Briefs*, vol. 66, no. 7, pp. 1154–1158, Jul. 2019.

[5] J. Shi, J. Wang, K. Xu, J.-X. Chen, and W. Liu, "A balanced-to-balanced power divider with wide bandwidth," *IEEE Microw. Wireless Compon. Lett.*, vol. 25, no. 9, pp. 573–575, Sep. 2015.

[6] H. Zhu, J. –Y. Lin, and Y. J. Guo, "Single-ended-to-balanced power divider with extended common-mode suppression and its application to differential Butlermatrices",*IEEE Trans. Microw. Theory Techn.*, vol. 68, no. 4, pp. 1510–1519, Apr. 2020.

[7] F. Lin, "A planar balanced quadrature coupler with tunable powerdividing ratio," *IEEE Trans. Ind. Electron.*, vol. 65, no. 8, pp. 6515–6526, Aug. 2018.

[8] W. Feng, Y. Zhao, W. Che, R. Gómez-García, and Q. Xue, "Multi-band balanced couplers with broadband common-mode suppression," *IEEE Trans. Circuits Syst., II, Exp. Briefs*, vol. 65, no. 12, pp. 1964–1968, Dec. 2018.

[9] L. –L.Qiu, L. Zhu, Y.-P.Lyu, "Balanced wideband phase shifters with wide phase shift range and good common-mode suppression", *IEEE Trans. Microw. Theory Techn.*,vol. 67, no. 8, pp. 3403-3413, 2019.

[10] A. N. Yadav, and R. Bhattacharjee, "Balanced to unbalanced powerdivider with arbitrary power ratio," *IEEE Microw. Wireless Compon.* Lett., vol. 26, no. 11, pp. 885–887, Nov. 2016

[11] J. Shi, K. Xu, J. Lu, and J.-X. Chen, "A coupled-line balanced-to-single-ended out-of-phase power divider with enhanced bandwidth," *IEEE Trans. Microw. Theory Techn.*, vol. 65, no. 2, pp. 2561–2569, Feb. 2017.

[12] S. Chen, W. –C. Lee, and T. –L. Wu, "balanced-to-balanced and balanced-to-unbalanced power dividers with ultra-wideband common-mode rejection and absorption based onmode-conversion approach," *IEEE Trans. Compon., Packag., Manuf. Technol.*, vol. 9, no. 2, pp. 306–316, Feb. 2019.

[13] K. Xu, J. Shi, L. L. Lin, and J.-X. Chen, "A balanced-to-unbalanced microstrip power divider with filtering function," *IEEE Trans. Microw. Theory Techn.*, vol. 63, no. 8, pp. 2561–2569, Aug. 2015.

[14] X. Gao, W. Feng, W. Che, and Q. Xue, "Wideband balanced-to-unbalanced filtering power dividers based on coupled lines," *IEEE Trans. Microw. Theory Techn.*, vol. 65, no. 1, pp. 86–95, Jan. 2017.

[15] H. Zhu, J. Y. Lin and Y. J. Guo, "Filtering balanced-to-single-ended power dividers with wide range and high level of common-mode suppression," *IEEE Trans. Microw. Theory Techn.*, vol. 67, no. 12, pp. 5038–5048, Dec. 2019.

[16] W. Feng, M. Hong, and W. Che, "Dual-band balanced-to-unbalanced filtering power divider by coupled ring resonators," *Electron. Lett.*, vol. 52, no. 22, pp. 1862-1864, Oct. 2016.

[17] Z. Zhuang, Y. Wu, M. Kong, W. Wang, and Y. Liu, "Dual-band filtering balanced-to-unbalanced impedance-transforming power divider with high frequency ratio and arbitrary power division," *IEEE Access*, vol. 6, pp. 12710-12717, 2018.

[18] F. Huang, J. Wang, J. Hong, and W. Wu, ''A new balanced-to-unbalanced filtering power divider with dual controllable passbands and

enhanced inband common-mode suppression,'' *IEEE Trans. Microw. Theory Techn.*, vol. 67, no. 2, pp. 695–703, Feb. 2019.

[19] H. Liu, Z. Wang, S. Hu, H. –X. Xu, and B. Ren, "Design of tri-band balanced filter with wideband common-mode suppression and upper stopband using square ring loaded resonator", *IEEE Trans. Circuits Syst. II, Exp. Briefs*, to be published. DOI: 10.1109/TCSII.2019.2949772.

[20] F. Wei, P. Y. Qin, Y. J. Guo, C. Ding, and X. W. Shi, "Compact balanced dual- and tri-band BPFs based on coupled complementary split-ring resonators (C-CSRR)," *IEEE Microw. Wireless Compon. Lett*., vol. 26, no. 2, pp. 107–109, Feb. 2016.